Article:
Andrews, T, Gregory, JM, Paynter, D et al. (2018) Accounting for Changing Temperature Patterns Increases Historical Estimates of Climate Sensitivity. Geophysical Research Letters, 45 (16). pp. 8490-8499. ISSN: 0094-8276

https://doi.org/10.1029/2018GL078887

Accounting for changing temperature patterns increases historical estimates of climate sensitivity

Timothy Andrews[1#], Jonathan M. Gregory[1,2], David Paynter[3], Levi G. Silvers[4], Chen Zhou[5], Thorsten Mauritsen[6], Mark J. Webb[1], Kyle C. Armour[7], Piers M. Forster[8] and Holly Titchner[1].

[1]Met Office Hadley Centre, Exeter, UK.
[2]NCAS-Climate, University of Reading, Reading, UK.
[3]GFDL-NOAA, Princeton, USA.
[4]Princeton University / GFDL, Princeton, USA.
[5]Nanjing University, China.
[6]Max Planck Institute for Meteorology, Hamburg, Germany.
[7]University of Washington, Seattle, USA.
[8]School of Earth and Environment, University of Leeds, Leeds, UK.

Submitted: 23rd May 2018
Revised: 10th July 2018

Key points

- Climate sensitivity simulated for observed surface temperature change is smaller than for long-term carbon dioxide increases.
- Observed historical energy budget constraints give climate sensitivity values that are too low and overly constrained, particularly at the upper end.
- Historical energy budget changes only weakly constrain climate sensitivity.

[#]Corresponding Author:
Timothy Andrews
Met Office Hadley Centre
FitzRoy Road
Exeter, EX1 3PB.
E-mail: timothy.andrews@metoffice.gov.uk

Abstract

Eight Atmospheric General Circulation Models (AGCMs) are forced with observed historical (1871-2010) monthly sea-surface-temperature (SST) and sea-ice variations using the AMIP II dataset. The AGCMs therefore have a similar temperature pattern and trend to that of observed historical climate change. The AGCMs simulate a spread in climate feedback similar to that seen in coupled simulations of the response to CO_2 quadrupling. However the feedbacks are robustly more stabilizing and the effective climate sensitivity (EffCS) smaller. This is due to a 'pattern effect' whereby the pattern of observed historical SST change gives rise to more negative cloud and LW clear-sky feedbacks. Assuming the patterns of long-term temperature change simulated by models, and the radiative response to them, are credible, this implies that existing constraints on EffCS from historical energy budget variations give values that are too low and overly constrained, particularly at the upper end. For example, the pattern effect increases the long-term Otto et al. (2013) EffCS median and 5-95% confidence interval from 1.9K (0.9-5.0K) to 3.2K (1.5-8.1K).

Plain text summary

Recent decades have seen cooling over the eastern tropical Pacific and Southern Ocean while temperatures rise globally. Climate models indicate that these regional features, and others, are not expected to continue into the future under sustained forcing from atmospheric carbon dioxide increases. This matters, because climate sensitivity depends on the pattern of warming, so if the past has warmed differently from what we expect in the future then climate sensitivity estimated from the historical record may not apply to the future. We investigate this with a suite of climate models and show that climate sensitivity simulated for observed historical climate change is smaller than for long-term carbon dioxide increases. The results imply that historical energy budget changes only weakly constrain climate sensitivity.

1. Introduction

The relationship between global surface temperature change and the Earth's radiative response - a measure of the radiative feedbacks in the system and a key determinant of the Earth's climate sensitivity - can vary on timescales of decades to millennia. Thus feedbacks governing warming over the observed historical record may be different from those acting on the Earth's long-term climate sensitivity to rising greenhouse gas concentrations (e.g. Gregory and Andrews 2016; Zhou et al., 2016; Armour 2017; Proistosescu and Huybers 2017; Silvers et al., 2018; Marvel et al., 2018). This is in contrast to decades of studies that explicitly or implicitly assume that the relationship between historical temperature change and energy budget variations provides a direct constraint on long-term climate sensitivity (e.g. Gregory et al., 2002; Otto et al., 2013).

The primary reason why radiative feedback and sensitivity is not constant is because climate feedback depends on the spatial structure of surface temperature change (Armour et al. 2013; Rose et al., 2014; Andrews et al., 2015; Zhou et al. 2016; 2017; Haugstad et al., 2017; Ceppi and Gregory, 2017; Andrews and Webb, 2018; Silvers et al., 2018). This evolves on annual to decadal timescales with modes of unforced coupled atmosphere-ocean variability (e.g. Xie et al., 2016) and spatiotemporal variations in anthropogenic or natural forcings (e.g. Takahashi and Watanabe, 2016; Smith et al., 2016). It also evolves on decadal to centennial timescales in response to sustained anthropogenic forcing due to the intrinsic timescales of the climate response (such as delayed warming in the eastern tropical Pacific and Southern Ocean) (e.g. Senior and Mitchell, 2000; Andrews et al., 2015; Armour et al., 2016). Thus the pattern of historical temperature change, and thus radiative feedback, is expected to be different from that in response to long-term CO_2 increases (see Discussion). We refer to the dependency of radiative feedbacks on the evolving pattern of surface temperature change as a 'pattern effect' (Stevens et al., 2016).

Most previous estimates of climate sensitivity based upon historical observations of Earth's energy budget have not allowed for a pattern effect between historical climate change and the long-term response to CO_2 (e.g. Otto et al., 2013). Armour (2017) found that the equilibrium climate sensitivity (ECS) (the equilibrium near surface-air-temperature change in response to a CO_2 doubling) of Atmosphere-Ocean General Circulation Models (AOGCMs) (estimated from simulations of abrupt CO_2 quadrupling (*abrupt-4xCO2*)) was about 26% larger than climate sensitivity inferred from transient warming (1%CO2 simulations, taken to be an analogue for historical climate change) due to pattern effects. Armour (2017)

therefore concluded that energy budget estimates of Earth's ECS from the historical record should be increased by this amount. Lewis and Curry (2018) argue for a smaller pattern effect, highlighting ambiguities in the methodology when using idealised CO_2 experiments as an analogue for historical climate change. However, as noted in Armour (2017), the use of 1%CO2 simulations as an analogue for historical climate change has important limitations in that it neglects the impact from non-CO_2 forcings and unforced climate variability that could have had a significant impact on the pattern of historical temperature change. In particular, under 1%CO2, AOGCMs do not show cooling of the tropical eastern Pacific Ocean and Southern Ocean – features that have been observed over recent decades but are not expected in the long-term response to increased CO_2 (Zhou et al., 2016). These are regions where atmospheric feedbacks (in particular clouds) are sensitive to the patterns of surface temperature change due to their impact on local and remote atmospheric stability (e.g. Zhou et al., 2017; Andrews and Webb, 2018). This suggests that the magnitude of the pattern effect reported in Armour (2017) may be too low relative to historical climate change. This is an outstanding issue that we aim to address and quantify here.

Here we will show that a suite of Atmospheric General Circulation Models (AGCMs) forced with historical (post 1870) sea-surface-temperatures (SSTs) and sea-ice changes are ideal simulations for quantifying the relationship between historical climate sensitivity and idealised long-term model derived ECS. They allow us, for the first time, to quantify the pattern effect associated with observed temperature patterns, and so provide improved updates to estimates of climate sensitivity derived from historical energy budget constraints. The work builds upon individual studies (Andrews, 2014; Gregory and Andrews 2016; Zhou et al., 2016; Silvers et al., 2018). Our aim is to: (i) bring together these individual model results for an intercomparison of AGCMs forced with historical SST and sea-ice variations; (ii) explore the dependence of the experimental design to the underlying SST and sea-ice dataset; (iii) explore how historical feedbacks in the AGCMs relate to feedbacks diagnosed from their parent AOGCM forced by *abrupt-4xCO2*; (iv) quantify the pattern effect causing the difference between climate sensitivity under historical climate change and long-term CO_2 changes; (v) use this pattern effect to update observed energy budget constraints on Earth's climate sensitivity.

2. Simulations, Models and Data

Eight AGCMs (Table 1) are forced with monthly time-varying observationally derived fields of SST and sea-ice from 1871 to 2010 using the Atmospheric Model Intercomparison Project

(AMIP) II boundary condition data set (Gates et al., 1999; Taylor et al., 2000; Hurrell et al., 2008). All simulations have natural and anthropogenic forcings (e.g. greenhouse gases, aerosols, solar radiation etc.) held constant at assumed pre-industrial conditions (except CAM4 which used assumed constant present-day conditions; we assume the level of background forcing has no impact on the diagnosed feedback of the model). With *constant* forcings the variation in radiative fluxes comes about solely from the changing SST and sea-ice boundary conditions, allowing radiative feedbacks to be accurately diagnosed directly from top-of-atmosphere (TOA) radiation fields (e.g. Haugstad et al., 2017). For details of individual simulations see Gregory and Andrews (2016) for HadGEM2 and HadAM3, Silvers et al. (2017) for GFDL-AM2.1, GFDL-AM3 and GFDL-AM4.0, Zhou et al. (2016) for CAM4 and CAM5.3, and Mauritsen et al. (2018) for ECHAM6.3. This experiment, referred to here as *amip-piForcing* (Gregory and Andrews, 2016), is included in the Cloud Feedback Model Intercomparison Project (CFMIP) contribution to CMIP6 (Webb et al. 2017). The sensitivity of the results to the AMIP II boundary condition dataset is explored with analogous experiments using the HadISST2.1 SST and sea-ice dataset (Titchner and Rayner, 2014) (Supporting Information).

All simulations ran for 140yrs from Jan 1871 through to Dec 2010, except for GFDL-AM2.1 and GFDL-AM3 which finished in Dec 2004. All data is global-annual-mean and anomalies are presented relative to an 1871-1900 baseline. CAM4 and CAM5.3 results are single realisations, HadGEM2 and HadAM3 simulations are ensembles of 4 realisations each, ECHAM6.3, GFDL-AM2.1 and GFDL-AM4.0 have 5 realisations each, while GFDL-AM3 has 6 realisations. The HadGEM2 results are not identical to those presented in Gregory and Andrews (2016) because it has been discovered that land-cover change was included in their HadGEM2 simulations. We have confirmed that the updated simulations used here, which have constant land-cover, do not affect the main conclusions of Gregory and Andrews (2016). In fact the multi-decadal variability in feedback in HadGEM2 is now found to be more consistent with their HadAM3 results (Section 3).

For comparison to long-term climate sensitivity and feedback parameters we make use of an *abrupt-4xCO2* simulation of each AGCM's parent AOGCM. For CAM4, GFDL-AM2.1, GFDL-AM3 and HadGEM2 we use the CCSM4, GFDL-ESM2M, GFDL-CM3 and HadGEM2-ES CMIP5 *abrupt-4xCO2* simulations respectively (Taylor et al., 2012). Feedbacks and associated e*ffective* climate sensitivity (EffCS) (the equilibrium near surface-air-temperature change in response to a CO_2 doubling assuming constant feedback strength) are derived from the regression of global-annual-mean change in radiative flux dN against surface-air-temperature change dT for the 150yrs of the simulation, according to EffCS=$-F_{2x}/\lambda$, where

F_{2x}, the forcing from a doubling of CO_2, is equal to the dN-axis intercept divided by two (to convert 4xCO_2 to 2xCO_2) and λ, the feedback parameter, is equal to the slope of the regression line (Andrews et al., 2012). We have similar simulations for ECHAM6.3 and HadAM3 using the MPI-ESM1.1 and HadCM3 models respectively, though these are not in the CMIP5 archive. The HadCM3 simulation is only 100yrs long but is a mean of 7 realisations. CAM5.3 and GFDL-AM4.0 do not yet have equivalent coupled 4xCO_2 simulations. We choose to use EffCS rather than the 'true' *equilibrium* climate sensitivity (ECS) since few AOGCMs are run to equilibrium and thus the true ECS is not generally known. Paynter et al. (2018) showed that the actual ECS from multimillennial GFDL-ESM2M and GFDL-CM3 simulations was nearly 1K higher than the EffCS we use here from *abrupt-4xCO2*. Hence the values we report for EffCS might be viewed as a lower bound on ECS if other models behave in a similar way.

3. Radiative feedbacks and sensitivities

Figure 1a shows the global-annual-mean near-surface-air-temperature change (dT) of the eight individual AGCM *amip-piForcing* simulations in comparison to HadCRUT4 (Morice et al., 2012). As expected the models capture the observed variability and trends in dT well (the correlation coefficient, r, between observed and simulated dT is >0.95 for every model). However the AGCMs omit the small part of the recent warming trend over land that arises as a direct adjustment to changes in CO_2 and other forcing agents (dT in HadCRUT4 averaged over 2000-2010 is 0.79K, whereas it ranges from 0.66-0.76K in the AGCMs) (see also, Andrews, 2014; Gregory and Andrews, 2016). Figure 1b shows the net TOA radiative flux change, dN. It is generally negative because as dT increases positively the planet loses heat to space. This relationship is shown in Figure 1c for the multi-model ensemble-mean. The slope of the regression line (ordinary least-squares, over the annual-mean 1871-2010 timeseries data) measures the feedback parameter λ_{amip} (in Wm^{-2} K^{-1}), where subscript 'amip' is used to indicate that the feedback parameter was derived from the *amip-piForcing* experiment. Individual model results are given in Table 1.

The equivalent feedback parameters derived from six available parent AOGCM *abrupt-4xCO2* simulations (λ_{4xCO2}) are compared to λ_{amip} in Figure 2 and Table 1. We find that λ_{amip} is more negative than λ_{4xCO2} in all models. In other words, AGCMs forced with historical SST and sea-ice changes robustly simulate more stabilizing feedbacks (lower EffCS) than their parent AOGCM forced by long-term CO_2 changes. On average, the difference in λ between

196 *amip-piForcing* and *abrupt-4xCO2* is $\Delta\lambda=\lambda_{4xCO2}-\lambda_{amip}=0.64$ Wm^{-2} K^{-1}, ranging from 0.29 to
197 1.04 Wm^{-2} K^{-1} across the AGCMs (Table 1).
198
199 The source of $\Delta\lambda$ is shown in Figure 2. The clear-sky feedback (Figure 1d,e) is slightly (but
200 robustly) more negative in *amip-piForcing* compared to *abrupt-4xCO2* (Figure 2b) due to
201 differences in LW clear-sky feedback processes that are partly offset by SW clear-sky
202 feedback differences (Figure 2d). This difference in clear-sky alone explains the relatively
203 small change in net sensitivity for the GFDL-AM2.1 model. For the other models, differences
204 in cloud feedback (Figure 1f) are a larger source of the reduced sensitivity in *amip-piForcing*
205 (Figure 2c). This mostly comes from SW cloud feedback processes, with historical LW cloud
206 feedback processes generally being representative of that seen in *abrupt-4xCO2* (Figure
207 2e). These findings are consistent with process orientated studies that suggest lapse-rate
208 (which affects LW clear-sky) and low-cloud (which affect SW and NET CRE) feedbacks vary
209 the most with SST patterns, especially in the Pacific (see below and: Rose et al., 2014;
210 Andrews et al., 2015; Zhou et al., 2016; 2017; Silvers et al., 2017; Ceppi and Gregory, 2017;
211 Andrews and Webb, 2018).
212
213 In *amip-piForcing* the model-mean $EffCS_{amip}=-F_{2x}/\lambda_{amip}$ is ~2K, ranging from 1.6 to 2.2K
214 across the AGCMs (Table 1). The narrowness of this $EffCS_{amip}$ range does not arise due to
215 reduced uncertainty in λ_{amip} relative to λ_{4xCO2}. On the contrary, the spread (measured by
216 1.645*σ) in λ_{amip} is almost the same size as the spread in λ_{4xCO2} (Table 1). The spread in
217 $EffCS_{amip}$ is narrower primarily because λ_{amip} is on average more negative than λ_{4xCO2}. Since
218 EffCS depends on the reciprocal of λ, the same spread in λ, shifted to more negative
219 numbers, will give rise to a narrower spread in EffCS (e.g., Roe, 2009). A similar spread in
220 in λ_{amip} and λ_{4xCO2} suggests that different patterns of SST change across AOGCMs do not
221 contribute significantly to the spread in atmospheric feedbacks in *abrupt-4xCO2* experiments
222 (see also Ringer et al., 2014; Andrews and Webb, 2018), which must therefore come about
223 due to differences in atmospheric physics and parameterisations.
224
225 $EffCS_{4xCO2}$ (of the parent AOGCM) is in all cases larger than $EffCS_{amip}$, ranging from 2.4 to
226 4.6K (Table 1). In the multi-model-mean, $EffCS_{4xCO2}$ is ~67% larger than that implied from
227 $EffCS_{amip}$. This model-mean historical pattern effect is substantially larger than the 26%
228 found by Armour (2017), supporting the hypothesis that the pattern effect is larger in the
229 historical record than simulated in transient 1%CO_2 AOGCM simulations because the later
230 miss key features of the observed warming pattern. This result is even more striking given
231 that Armour (2017) used an EffCS definition from *abrupt-4xCO2* that gives larger values than
232 ours (they used years 21-150 of *abrupt-4xCO2*, whereas we use years 1-150).

It is also useful to study shorter time periods to help inform our understanding of the relationship between shorter term variations in temperature and radiative fluxes, as have been used by many studies to estimate EffCS particularly since the satellite era (e.g. Forster, 2017). Figure 2f shows the feedback parameter for 30yr moving windows over the historical period in the AGCM simulations (calculated as per Gregory and Andrews, 2016), in comparison to λ_{4xCO2} (horizontal lines). There is substantial multi-decadal variability in the feedback parameter that is common to all models, with a peak in feedback parameter (higher EffCS) around the 1940s and a minimum (lower EffCS) in the most recent decades (post ~1980). Generally λ_{amip} is always more negative than λ_{4xCO2}. There are only a few instances where the λ_{amip} is similar to λ_{4xCO2}, for example ~1940 for HadGEM2 and GFDL-AM2.1, but no instances where λ_{amip} is substantially less negative than λ_{4xCO2}. The difference is greatest in the most recent decades, suggesting that energy budget constraints on ECS based on recent decades of satellite data will be most strongly biased low. This is consistent with process understanding of the pattern effect, since recent decades have shown substantial cooling in the eastern Pacific and Southern Ocean while warming in the west Pacific warm pool (e.g. Zhou et al., 2016). The cooling in the descent region of the tropical Pacific will favour increased cloudiness (a negative feedback), while warming in the west Pacific ascent region efficiently warms free tropospheric air (increasing the negative lapse-rate feedback widely across the tropics and mid-latitudes) as well as further increasing the lower tropospheric stability and cloudiness in the marine low-cloud descent regions (Zhou et al., 2016; Ceppi and Gregory, 2017; Andrews and Webb, 2018).

Most of the multi-decadal variation in feedback strength comes from changes in the strength of cloud feedback (the correlation between the Net and CRE feedback timeseries, calculated in a similar way, is >0.94 in each AGCM) while the clear-sky feedbacks show less variation (not shown). This, as well as atmospheric variability, helps explain why cloud feedback is not as linearly correlated to dT variations over the full historical period compared to clear-sky feedbacks (r=0.48 for CRE compared to 0.99 and 0.93 for the clear-sky fluxes, Figures 1d,e,f).

4. Constraints on observed estimates of climate sensitivity

The pattern effect causing the difference between simulated EffCS under historical climate change and long-term CO_2 increase implies that historical energy budget constraints on

EffCS do not directly apply to long-term ECS. To account for this, we use the difference in λ between *amip-piForcing* and *abrupt-4xCO2* as a measure of the pattern effect to update historical energy budget estimates of λ and EffCS. This is in contrast to Armour (2017) who had to use 1%CO2 simulations as a surrogate for historical climate change. Here we are quantifying the pattern effect associated with patterns of temperature change that actually occurred in the real world, relative to those simulated by AOGCMs to long-term CO_2 increases. The pattern effect therefore assumes that long-term warming patterns in AOGCMs not yet seen in the historical record, and the radiative response to them, are credible (see Discussion).

To illustrate the impact of the pattern effect we use the Otto et al. (2013) historical energy budget constraints as our starting point, though other datasets exist (see Forster, 2017) and clearly the EffCS estimates presented below will depend on this. First, we reproduce the historical EffCS estimates reported in Otto et al. (2013) using their best estimate and 5-95% confidence intervals for the historical (denoted by subscript 'hist') change in temperature (dT_{hist}=0.48±0.2 K), heat uptake (dN_{hist}=0.35±0.13 Wm^{-2}) and radiative forcing (dF_{hist}=1.21±0.52 Wm^{-2}) for the 40 yr period 1970-2009 relative to pre-industrial (which they define as 1860-1879) (their Table S1, row 5). To be consistent with Otto et al. (2013) we also use their forcing and its uncertainty for a doubling of CO_2 (F_{2x}=3.44 (±10%) Wm^{-2}). We randomly sample (with replacement) 10 million times from the gaussian distributions of dT_{hist}, dN_{hist}, dF_{hist} and F_{2x} to calculate $\lambda_{hist}= (dN_{hist}-dF_{hist})/dT_{hist}$ and $EffCS_{hist}=-F_{2x}/\lambda_{hist}$. We assume the uncertainty in F_{2x} and the greenhouse gas component of dF_{hist} are correlated as in Otto et al. (2013). The resulting EffCS values are binned into intervals of 0.02 and normalised to produce a probability density function (PDF), excluding values less than zero and greater than twenty. The resulting PDF and percentiles (Figure 3, black lines) recovers the Otto et al. (2013) $EffCS_{hist}$ median (1.9K) and 5-95% confidence interval (0.9-5.0K) to within 0.1K.

Following Armour (2017), we update the Otto et al. (2013) EffCS estimate for the pattern effect between historical climate change and abrupt-4xCO2 using two methods. We first scale the historical feedback parameter λ_{hist} by the ratio of the feedbacks found in the *amip-piForcing* and *abrupt-4xCO2* simulations, so $\lambda=\lambda_{hist}*S$ where $S=\lambda_{4xCO2}/\lambda_{amip}$ (Table 1). EffCS is then given by $EffCS=-F_{2x}/\lambda=-F_{2x}/(\lambda_{hist}*S)$ (equivalent to Equation 4 in Armour 2017). Alternatively, we update λ_{hist} by the difference in feedbacks, according to $\lambda=\lambda_{hist}+\Delta\lambda$, where $\Delta\lambda=\lambda_{4xCO2}-\lambda_{amip}$. EffCS is then given by $EffCS=-F_{2x}/\lambda=-F_{2x}/(\lambda_{hist}+\Delta\lambda)$ (equivalent to Equation 5 in Armour 2017). We then calculate the EffCS PDF as above by randomly sampling from the F_{2x} and λ_{hist} distributions, along with S and $\Delta\lambda$ chosen randomly with equal likelihood from the individual model results (Table 1). Note that using the difference ($\Delta\lambda$) approach

increases the likelihood of returning very large (or even negative) EffCS values, since $\lambda=\lambda_{hist}+\Delta\lambda$ can result in λ values close to zero or even with a changed sign when sampling λ_{hist} values that are small. Hence the results of this method are potentially sensitive to the assumption of excluding negative EffCS values or those greater than 20K.

We compare the PDF of $EffCS_{hist}$ (which is an approximation of Otto et al. (2013)) against its updated versions that accounts of the pattern effect in Figure 3. The Otto et al. (2013) median and 5-95% confidence interval increases from 1.9K (0.9-5.0K) to 3.2K (1.5-8.1K) using the ratio (*S*) approach (Figure 3, red lines), or 2.7K (1.1-10.2K) if we use the difference ($\Delta\lambda$) approach (Figure 3, blue lines). Alternatively, if we take the Otto et al. (2013) data relating to their most recent decade (2000-2009) (their Table S1 row 4) then the Otto et al. (2013) estimate and 5-95% confidence interval increases from 2.0K (1.2-3.9K) to 3.3K (1.8-6.8K) using the ratio approach or 3.0K (1.5-9.7K) using the difference approach. Thus, eitherway and for different time periods, the pattern effect from *amip-piForcing* to *abrupt-4xCO2* results in a substantial median ECS increase, while the lowest values of ECS become less likely, and higher ECS values become much harder to rule out.

Another way of estimating the pattern effect is by comparing feedbacks in AOGCM historical simulations to *abrupt-4xCO2* (e.g. Paynter and Frolicher, 2015; Marvel et al., 2018). However we believe *amip-piForcing* is superior, because (i) the diagnosed pattern effect in an AOGCM historical simulation will depend on its ability to correctly simulate the patterns of historical climate change, including the magnitude and timing of unforced variability, which they are not expected to simulate correctly (e.g. Zhou et al., 2016; Mauritsen, 2016) and (ii) determining feedbacks in AOGCM historical simulations requires knowledge of the time-varying effective radiative forcing of the model, something which is not routinely diagnosed and is difficult to assume because of model diversity in forcing, particularly from aerosols (Forster, 2017). The *amip-piForcing* approach alleviates both of the above issues.

Note that for simplicity in the above calculations we have assumed that λ_{amip} (calculated via linear regression over the *amip-piForcing* simulations, Section 3) is appropriate to the time periods and methodology of Otto et al. (2013) (who use finite differences, rather than linear regression, between decades to calculate changes). To check this we recompute λ_{amip} and the corresponding *S* and $\Delta\lambda$ values using the same method and time-periods as Otto et al., i.e. $\lambda_{amip}=dN/dT$, where dN and dT are averaged over the relevant decades (though for 2000-2009 we use the 1995-2004 decade, since the GFDL runs finished in 2004). We cannot use an identical baseline as Otto et al. (2013) since our simulations begin in 1871 and their baseline begins in 1860. Regardless, for 1979-2009 or 2000-2009, the resulting updated

EffCS PDF has a median and 5-95% confidence interval to within ±15% of the regression methods used above. Hence in practice our conclusions are not sensitive on this assumption.

5. Summary and discussion

An intercomparison of AGCMs forced with historical (post 1870) sea-surface-temperatures and sea-ice from the AMIP II boundary condition dataset reveal some common results:

1. When AGCMs are forced with historical SST and sea-ice changes the models agree on an effective climate sensitivity (EffCS) of ~2K, in line with best estimates from historical energy budget variations (e.g. Otto et al., 2013) but significantly lower than the EffCS of the corresponding parent AOGCMs when forced with *abrupt-4xCO_2* (~2.4 - 4.6K for the corresponding set of models).

2. The lower historical EffCS relative to *abrupt-4xCO2* is predominantly because LW clear-sky and cloud radiative feedbacks are less positive in response to historical SST and sea-ice variations than in long-term climate sensitivity simulations. This is an example of what is called a 'pattern effect' (Stevens et al., 2016), and is consistent with process understanding that suggests lapse-rate and low-cloud feedbacks vary most with SST patterns, especially those in the tropical Pacific ascent/descent regions which have large impacts on atmospheric stability (Zhou et al., 2016; Ceppi and Gregory, 2017, Andrews and Webb, 2018).

3. The models agree that the most recent decades (e.g. 1980-2010) generally give rise to the most negative feedbacks (lowest EffCS). Hence the pattern effect will be largest for estimates of feedbacks and EffCS based on the satellite era. This is a period when the eastern tropical Pacific and Southern Ocean, regions important for the pattern effect, have been cooling, but are not expected to continue to do so in the long-term response to increased CO_2 (e.g. Zhou et al., 2016).

The pattern effect causing the difference between EffCS under historical climate change and long-term CO_2 changes implies that current constraints on climate sensitivity that do not consider this give values that are too low and are overly constrained, particularly at the upper bound. We present an approach to adjust historical energy budget derived EffCS estimates for the pattern effect. For example, the historical (1860-1879 to 1970-2009)

observational EffCS estimate (median) and 5-95% confidence interval of Otto et al. (2013) increases from 1.9K (0.9-5.0K) to 3.2K (1.5-8.1K) using an approach that scales the historical feedback parameter by the ratio of the feedbacks found in *amip-piForcing* and *abrupt-4xCO2*. Thus the pattern effect increases historical EffCS median values, reduces the likelihood of the lowest EffCS values, and makes higher values significantly harder to rule out. Determining whether values towards the extremes of these bounds are plausible would require further understanding of the pattern effect or assessing and combining other lines of evidence, such as from process understanding (see Stevens et al., 2016). This is important because a higher EffCS increases the risk of state-dependent feedbacks and large warmings (Bloch-Johnson et al., 2015).

The pattern effect between historical climate change and long-term CO_2 increase assumes that key aspects of long-term warming patterns simulated by AOGCMs not yet seen in the observational record, such as substantial warming of the Southern Ocean and eastern tropical Pacific, and the radiative response to them, are credible. Such patterns are consistent with paleo records (e.g. Masson-Delmotte et al. 2013; Fedorov et al., 2015) and basic physical understanding of the behaviour and timescale of oceanic upwelling (e.g. Clement et al. 1996, Held et al., 2010; Armour et al., 2016), though they are difficult to observationally constrain (Mauritsen, 2016). To argue for a negligible pattern effect (e.g. Lewis and Curry, 2018) would require that atmospheric feedbacks are insensitive to patterns of temperature change, or that the pattern of observed historical temperature change represents the equilibrated pattern response to increased CO_2. This is at odds with basic physical understanding and bodies of work on the role for unforced variability, transient effects and non-CO_2 forcings such as aerosols on the pattern of historical climate change (e.g. Held et al., 2010; Jones et al., 2013; Xie et al., 2016; Takahasi and Watanabe, 2016; Armour et al., 2016). Further progress in constraining the pattern effect and EffCS will come from improved understanding of the causes and processes of surface temperature change patterns in observations and AOGCM projections, as well as the radiative response to them.

Acknowledgments and data

Global-annual timeseries data of temperature and radiative flux change in the *amip-piForcing* simulations, as well as the abrupt-4xCO2 simulations not in the CMIP5 archive, are provided in the Supporting Datasets. We thank Michael Winton, Tom Knutson, Mark Ringer, Gareth Jones and two anonymous reviewers for constructive comments. TA, JMG

and MJW were supported by the Met Office Hadley Centre Climate Programme funded by BEIS and Defra.. PMF was supported by grant NE/N006038/1.

References

Andrews, T., and M.J. Webb, 2018: The dependence of global cloud and lapse rate feedbacks on the spatial structure of tropical pacific warming. *J. Climate*, 31, 641–654, doi:10.1175/JCLI-D-17-0087.

Andrews, T., J.M. Gregory, and M.J. Webb, 2015: The dependence of radiative forcing and feedback on evolving patterns of surface temperature change in climate models, *J. Clim.*, 28, 1630–1648, doi:10.1175/jcli-d-14-00545.1.

Andrews, T., 2014: Using an AGCM to diagnose historical effective radiative forcing and mechanisms of recent decadal climate change, *J. Clim.*, 27, 1193–1209, doi:10.1175/jcli-d-13-00336.1.

Andrews, T., J.M. Gregory, M.J. Webb, and K.E. Taylor, 2012: Forcing, feedbacks and climate sensitivity in CMIP5 coupled atmosphere–ocean climate models, *Geophys. Res. Lett.*, 39, L09712.

Armour, K.C., 2017: Energy budget constraints on climate sensitivity in light of inconstant climate feedbacks, *Nature Climate Change*, 7, 331–335, doi:10.1038/nclimate3278.

Armour, K.C., J. Marshall, J.R. Scott, A. Donohoe and E.R. Newsom, 2016: Southern Ocean warming delayed by circumpolar upwelling and equatorward transport. *Nature Geoscience*, 9, 549–554, doi:10.1038/ngeo2731.

Armour, K.C., C.M. Bitz and G.H. Roe, 2013: Time-varying climate sensitivity from regional feedbacks. *J. Climate,* 26, 4518-4534, doi: 10.1175/JCLI-D-12-00544.1.

Bloch-Johnson, J., R.T. Pierrehumbert, and D S. Abbot, 2015: Feedback temperature dependence determines the risk of high warming. *Geophys. Res. Lett.*, 42, 4973–4980. doi: 10.1002/2015GL064240.

441 Ceppi, P., and J.M. Gregory, 2017: Relationship of tropospheric stability to climate sensitivity
442 and Earth's observed radiation budget. *PNAS*, 114(50), doi:10.1073/pnas.1714308114.
443
444 Clement, A.C., R. Seager, M.A. Cane and S.E. Zebiak (1996), An ocean dynamical
445 thermostat. *J. Climate*, 9, 2190–2196.
446
447 Collins, M., et al. (2013), Long-term climate change: Projections, commitments and
448 irreversibility, in Climate Change 2013: The Physical Science Basis. Contribution of Working
449 Group I to the Fifth Assessment Report of the Intergovernmental Panel on Climate Change,
450 edited by M. Collins et al., pp. 1029–1136, Cambridge Univ. Press.
451
452 Fedorov, A.V., N.J. Burls, K.T. Lawrence and L.C. Peterson, 2015: Tightly linked zonal and
453 meridional sea surface temperature gradients over the past five million years. *Nature*
454 *Geoscience,* 8, 975-980, doi:10.1038/ngeo2755.
455
456 Forster, P.M., 2017: Inference of Climate Sensitivity from Analysis of Earth's Energy Budget,
457 *Annu. Rev. Earth Planet. Sci.*, 44, 85-106. doi: 10.1146/annurev-earth-060614-105156.
458
459 Gates, W.L., et al., 1999: An Overview of the Results of the Atmospheric Model
460 Intercomparison Project (AMIP I). *Bull. Amer. Meteor. Soc.*, 80, 29–56.
461
462 Gregory, J.M., and T. Andrews, 2016: Variation in climate sensitivity and feedback
463 parameters during the historical period. *Geophys. Res. Lett.*, 43, 3911–3920,
464 doi:10.1002/2016GL068406.
465
466 Gregory, J.M., R.J. Stouffer, S.C. Raper, P.A. Stott, and N.A. Rayner, 2002: An
467 Observationally Based Estimate of the Climate Sensitivity. *J. Climate*, 15, 3117–3121.
468
469 Haugstad, A. D., K. C. Armour, D. S. Battisti, and B. E. J. Rose (2017), Relative roles of
470 surface temperature and climate forcing patterns in the inconstancy of radiative feedbacks,
471 *Geophys. Res. Lett.*, 44, 7455–7463, doi:10.1002/2017GL074372.
472
473 Held, I.M., et al. (2010), Probing the fast and slow components of global warming by returning
474 abruptly to preindustrial forcing. *J. Climate*, 23, 2418-2427.
475

476 Hurrell, J., J. Hack, D. Shea, J. Caron, and J. Rosinski, 2008: A New Sea Surface
477 Temperature and Sea Ice Boundary Dataset for the Community Atmosphere Model. *J.*
478 *Climate*, 21, 5145–5153, doi: 10.1175/2008JCLI2292.1.
479
480 Jones, G. S., P. A. Stott, and N. Christidis (2013), Attribution of observed historical near–
481 surface temperature variations to anthropogenic and natural causes using CMIP5
482 simulations, *J. Geophys. Res. Atmos.*, 118, 4001–4024, doi: 10.1002/jgrd.50239.
483
484 Lewis, N. and J. Curry, 2018: The Impact of Recent Forcing and Ocean Heat Uptake Data
485 on Estimates of Climate Sensitivity. *J. Climate*, 31, 6051–6071, doi:10.1175/JCLI-D-17-
486 0667.1.
487
488 Marvel, K., Pincus, R., Schmidt, G. A., & Miller, R. L. (2018). Internal variability and
489 disequilibrium confound estimates of climate sensitivity from observations. *Geophysical*
490 *Research Letters*, 45, 1595–1601. https://doi.org/10.1002/2017GL076468.
491
492 Masson-Delmotte, V., et al. (2013), Information from paleoclimate archives, in Climate
493 Change 2013: The Physical Science Basis. Contribution of Working Group I to the Fifth
494 Assessment Report of the Intergovernmental Panel on Climate Change, edited by M. Collins
495 et al., pp. 383–464, Cambridge Univ. Press.
496
497 Mauritsen, T., et al., 2018: Developments in the MPI-M Earth System Model version 1.2
498 (MPI-ESM1.2) and its response to increase CO2. Submitted to *JAMES*.
499
500 Mauritsen, T., 2016: Global warming: Clouds cooled the Earth. *Nat. Geosci.*, 9, 865-867,
501 doi:10.1038/ngeo2838.
502
503 Otto., A., et al., 2013: Energy budget constraints on climate response. *Nature Geoscience*.
504 6, 415-416, doi:10.1038/ngeo1836.
505
506 Paynter, D., Frölicher, T. L., Horowitz, L. W., & Silvers, L. G. (2018). Equilibrium climate
507 sensitivity obtained from multimillennial runs of two GFDL climate models. *Journal of*
508 *Geophysical Research: Atmospheres*, 123, 1921–1941. doi:10.1002/2017JD027885.
509
510 Paynter, D., and T. L. Frölicher (2015), Sensitivity of radiative forcing, ocean heat uptake,
511 and climate feedback to changes in anthropogenic greenhouse gases and aerosols, *J.*
512 *Geophys. Res. Atmos.*, 120, 9837–9854, doi:10.1002/2015JD023364.

Proistosescu, C., and P.J. Huybers, 2017: Slow climate mode reconciles historical and model-based estimates of climate sensitivity. *Sci. Adv.*, 3, 7, doi:10.1126/sciadv.1602821.

Roe, G., 2009: Feedbacks, timescales, and seeing red. *Annu. Rev. Earth Planet. Sci.*, 37:93-115: doi: 10.1146/annurev.earth.061008.134734.

Rose, B.E.J., K.C. Armour, D.S. Battisti, N. Feldl, and D.D.B. Koll, 2014: The dependence of transient climate sensitivity and radiative feedbacks on the spatial pattern of ocean heat uptake, *Geophys. Res. Lett.*, 41, 1071–1078, doi:10.1002/2013GL058955.

Ringer, M.A., T. Andrews and M.J. Webb, 2014: Global-mean radiative feedbacks and forcing in atmosphere-only and fully-coupled climate change experiments. *Geophys. Res. Lett.*, 41, 4035-4042, doi:10.1002/2014GL060347.

Senior, C.A., and J.F.B Mitchell, 2000: The time-dependence of climate sensitivity. *Geophys. Res. Lett.*, 21(17), 2685-2688, doi:10.1029/2000GL011373.

Silvers, L.G., D. Paynter and M. Zhao, 2018: The diversity of cloud responses to twentieth century sea surface temperatures. *Geophysical Research Letters*, 45, 391–400. https://doi.org/10.1002/2017GL075583.

Smith, D.M., B.B.B. Booth, N.J. Dunstone, R. Eade, L. Hermanson, G.S. Jones, A.A Scaife, K.L. Sheen and V. Thompson, 2016: Role of volcanic and anthropogenic aerosols in the recent global surface warming slowdown. *Nature Climate Change.* 6, 936-940, doi:10.1038/nclimate3058.

Stevens, B., S.C. Sherwood, S. Bony, S. and M.J. Webb, 2016: Prospects for narrowing bounds on Earth's equilibrium climate sensitivity. *Earth's Future*, 4: 512-522. doi:10.1002/2016EF000376.

Takahashi, C., and M. Watanabe, 2016: Pacific trade winds accelerated by aerosol forcing over the past two decades. *Nature Climate Change*, 6, 768-772, doi:10.1038/nclimate2996.

Taylor, K. E., R. J. Stouffer, and G. A. Meehl, 2012: An overview of CMIP5 and the experiment design, *Bull. Am. Meteorol. Soc.*, 93, 485–498, doi:10.1175/bams-d-11-00094.1.

550 Taylor, K.E., D. Williamson, and F. Zwiers, 2000: The sea surface temperature and sea-ice
551 concentration boundary conditions for AMIP II simulations, PCMDI Report No. 60, Program
552 for Climate Model Diagnosis and Intercomparison, Lawrence Livermore National Laboratory.
553
554 Titchner, H. A., and N. A. Rayner (2014), The Met Office Hadley Centre sea ice and sea
555 surface temperature data set, version 2: 1. Sea ice concentrations, *J. Geophys. Res.*
556 *Atmos.*, 119, 2864–2889, doi:10.1002/2013JD020316.
557
558 Webb, M.J., et al., 2017: The Cloud Feedback Model Intercomparison Project (CFMIP)
559 contribution to CMIP6. Geosci. Model Dev., 10, 359-384, doi:10.5194/gmd-10-359-2017.
560
561 Xie., S-P., Y. Kosaka, and Y.M. Okumura, 2016: Distinct energy budgets for anthropogenic
562 and natural changes during global warming hiatus. *Nature Geoscience*. 9, 29-33,
563 doi:10.1038/ngeo2581.
564
565 Zhou, C., M. D. Zelinka, and S. A. Klein, 2017: Analyzing the dependence of global cloud
566 feedback on the spatial pattern of sea surface temperature change with a Green's function
567 approach. *J. Adv. Model. Earth Syst.*, 9, doi:10.1002/2017MS001096.
568
569 Zhou., C., M.D. Zelinka and S.A. Klein, 2016: Impact of decadal cloud variations on the
570 Earth's energy budget. *Nature Geoscience*, 9, 871-874, doi:10.1038/ngeo2828.

Tables

	λ_{amip}	λ_{4xCO2}	$S=\lambda_{4xCO2}/\lambda_{amip}$	$\Delta\lambda=\lambda_{4xCO2}-\lambda_{amip}$	$EffCS_{amip}$	$EffCS_{4xCO2}$
	(Wm^{-2} K^{-1})	(Wm^{-2} K^{-1})		(Wm^{-2} K^{-1})	(K)	(K)
CAM4	-2.27	-1.23	0.54	1.04	1.57	2.90
CAM5.3	-1.71	n/a	n/a	n/a	n/a	n/a
ECHAM6.3	-1.90	-1.36	0.72	0.54	2.17	3.01
GFDL-AM2.1	-1.67	-1.38	0.83	0.29	2.01	2.43
GFDL-AM3	-1.40	-0.75	0.53	0.65	2.13	3.99
GFDL-AM4.0	-1.91	n/a	n/a	n/a	n/a	n/a
HadAM3	-1.65	-1.04	0.63	0.61	2.14	3.38
HadGEM2	-1.37	-0.64	0.47	0.73	2.14	4.58
Mean(1.645*σ)	-1.74(0.48)	-1.07(0.52)	0.62(0.22)	0.64(0.40)	2.03(0.38)	3.38(1.29)

Table 1: Feedback parameters in *amip-piForcing* (λ_{amip}) and *abrupt-4xCO2* (λ_{4xCO2}) AGCM and AOGCM experiments. *S* and $\Delta\lambda$ are the ratio and differences between λ_{4xCO2} and λ_{amip} respectively. These are used to update feedback parameters derived from historical energy budget changes to account for the pattern effect between historical climate change and *abrupt-4xCO2*. $EffCS_{amip}=-F_{2x}/\lambda_{amip}$ and $EffCS_{4xCO2}=-F_{2x}/\lambda_{4xCO2}$ are the effective climate sensitivities from the *amip-piForcing* and *abrupt-4xCO2* experiments, where F_{2x} is the models effective radiative forcing for a doubling of CO2 (calculated from the *abrupt-4xCO2* experiments using a linear regression technique as per Andrews et al., 2012).

Figures

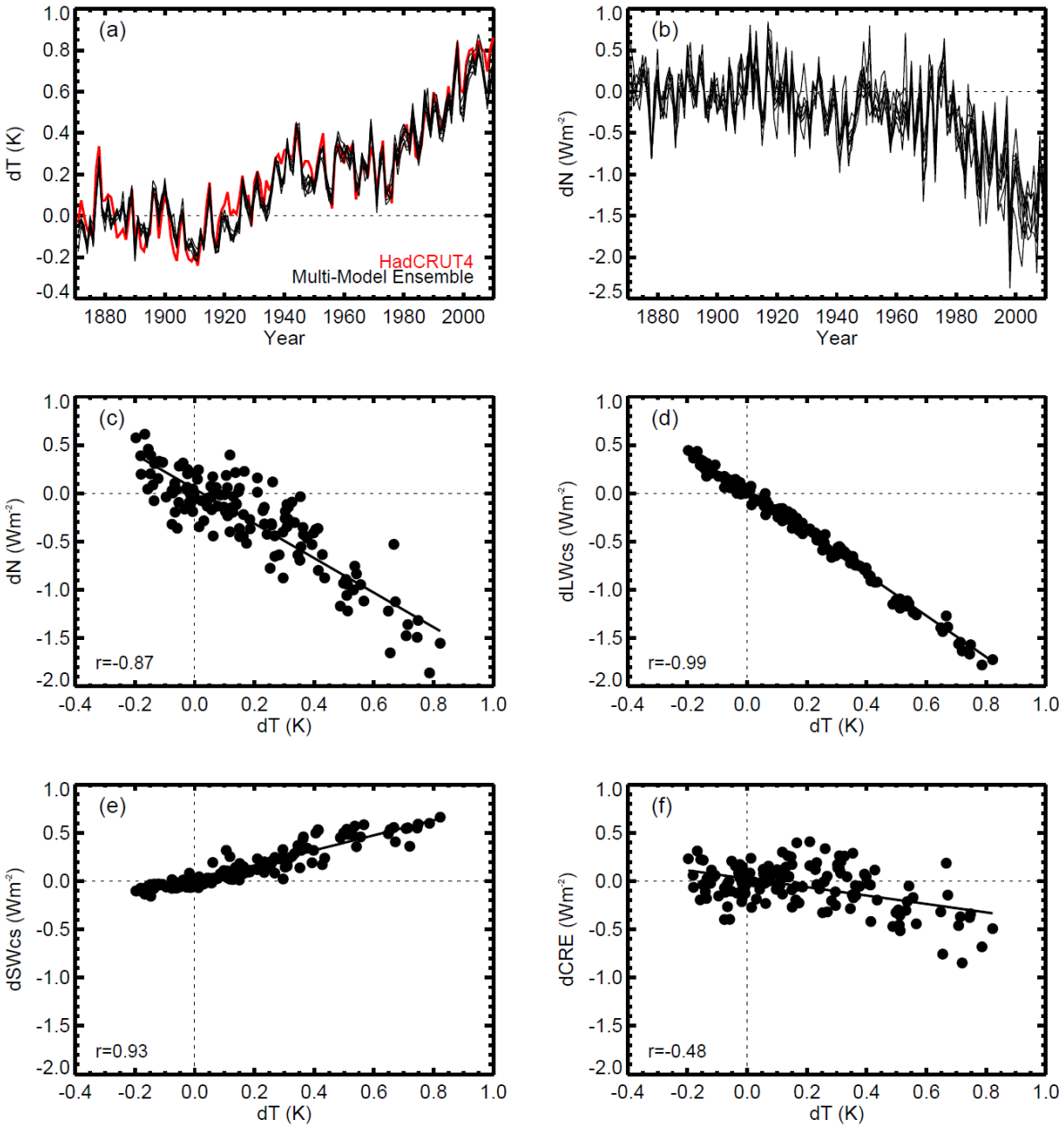

Figure 1: (a) Comparison of historical near-surface-air-temperature change (d*T*) simulated by the AGCMs in *amip-piForcing* (individual black lines) against observed (HadCRUT4) variations (red). (b) Timeseries of the change in net TOA radiative flux (d*N*) in the individual AGCM experiments. (c - f) The relationship and correlation coefficent (*r*) between the multi-model ensemble-mean (c) d*N*, (d) LW clear-sky radiative flux change, dLWcs, (e) SW clear-sky radiative flux change, dSWcs, and (f) cloud radiative effect change, dCRE, against d*T*. All points are global-annual-means covering the historical period (1871-2010) and fluxes are positive downwards. Changes are relative to an 1871-1900 baseline.

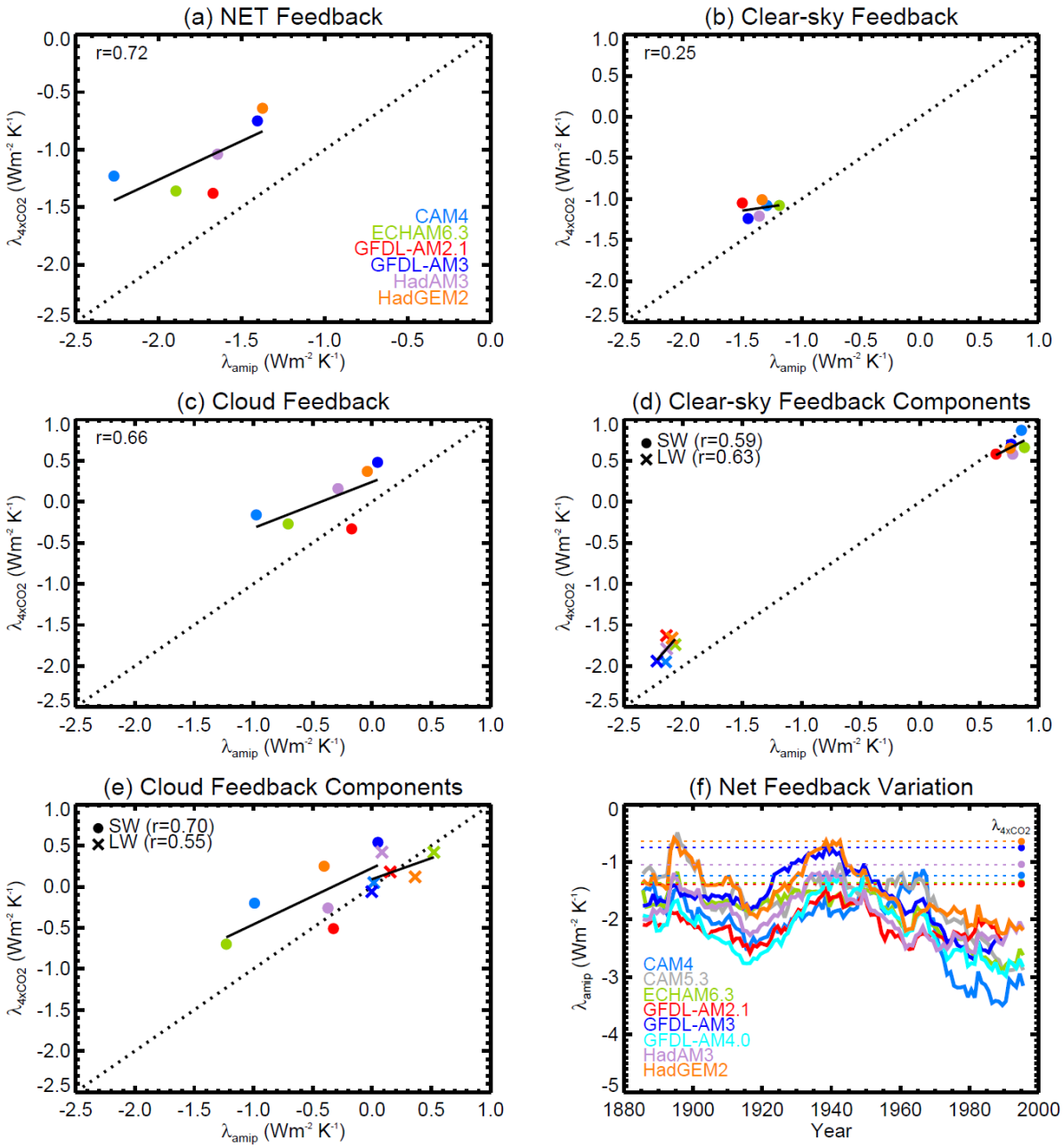

Figure 2: Relationship between the feedback parameter evaluated by regression of d*N* against d*T* over the historical period (1871-2010) in *amip-piForcing* (λ_{amip}) and 150yrs of abrupt-4xCO2 (λ_{4xCO2}) for (a) NET radiative feedback, (b) Clear-sky component, (c) CRE component, (d) LW and SW clear-sky components, (e) LW and SW CRE components. (f) Timeseries of λ_{amip} for individual AGCMs evaluated by linear regression of d*N* against d*T* in a sliding 30 year window in the *amip-piForcing* experiments, the year represents the centre of the window. Coloured circles in (f) with horizontal lines show the feedback parameter values from abrupt-4xCO_2.

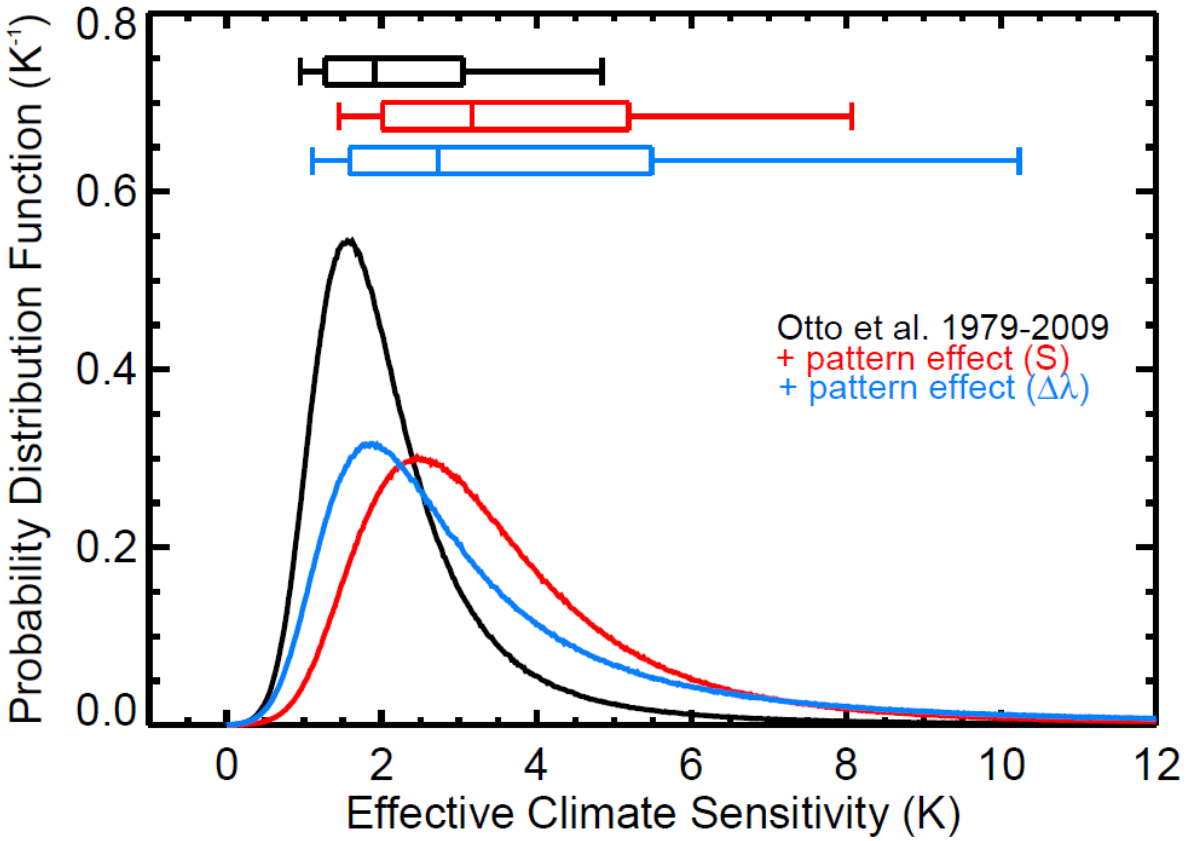

Figure 3: Comparison of the EffCS probability distribution function from a historical energy budget constraint (Otto et al, 2013), before (black) and after (colours) accounting for the pattern effect between historical climate change and abrupt-4xCO2. 'Red' accounts for the pattern effect by scaling the historical feedback parameter λ_{hist} by the ratio ($S=\lambda_{4xCO2}/\lambda_{amip}$) of the feedbacks found in the *amip-piForcing* and *abrupt-4xCO₂* simulations. 'Blue' accounts for the pattern effect by adding the difference in feedbacks ($\Delta\lambda=\lambda_{4xCO2}-\lambda_{amip}$) to λ_{hist} (see Section 4 and Table 1). Box plots show the 5-95% confidence interval (end bars), the 17-83% confidence interval (box ends) and the median (line in box).